ISSN 2464-4617 (print)
ISSN 2464-4625 (online) Computer Science Research Notes - CSRN http://www.wscg.eu

A Physics-Based Radiometric Simulator for Solar Localization and Heading Correction Validation in Off-Road Vehicles

Yann Duchemin*, Firas Jendoubi*†, Redouane Khemmar*
* Univ Rouen Normandie, ESIGELEC, Normandie Univ, IRSEEM UR4353, F-76000 Rouen, France
† SEGULA Technologies, 92000 Nanterre, France
Emails: yann.duchemin@irseem-esigelec.fr, firas.jendoubi@groupe-esigelec.org, redouane.khemmar@irseem-esigelec.fr

***Abstract*—Reliable heading estimation remains a major challenge for autonomous navigation in GNSS-denied (Global Navigation Satellite Systems) environments, where inertial navigation systems suffer from cumulative drift. The Sun provides a naturally available absolute reference, whose apparent position can be accurately predicted from astronomical models, but its observability is affected by complex radiometric, atmospheric, and optical phenomena. This paper proposes a physics-based radiometric simulator for validating solar-aided heading correction in off-road scenarios. The framework models the full observation chain, including solar irradiance, atmospheric transmittance, fisheye image formation, and sensor response, while environmental effects such as cloud coverage and visibility degradation are represented through parametric perturbations. The simulator enables controlled evaluation under degraded sensing conditions, including GNSS outages and inertial drift. Results show that solar-based correction reduces heading error accumulation and improves trajectory consistency by providing intermittent absolute orientation updates. The proposed approach serves as a proof-of-concept validation framework, highlighting the potential of physics-grounded simulation for resilient and low-cost navigation in challenging environments.**

***Index Terms*—Autonomous Navigation, Azimuth, Computer Vision, Physical Modeling, Solar Localization, Robotic Perception.**

I. Introduction

Reliable heading estimation remains a fundamental requirement for autonomous navigation, especially in off-road and GNSS-challenged environments where terrain irregularities and limited infrastructure degrade conventional localization pipelines. In such conditions, Global Navigation Satellite Systems (GNSS) may suffer from outages or severe degradation, while Inertial Measurement Units (IMUs), despite their short-term stability, accumulate drift over time. These limitations motivate the use of complementary absolute references to constrain long-term heading errors in a passive and low-cost manner.

Among naturally available references, the Sun is particularly attractive. Its apparent position can be predicted with high precision from astronomical ephemerides and provides an absolute orientation cue whenever observable. However, exploiting this signal in practice remains challenging, as it depends on complex radiometric and physical effects, including atmospheric attenuation, scattering, optical projection, sensor response, and environmental visibility. Consequently, validating solar-aided heading correction directly in real outdoor experiments is costly, difficult to reproduce, and poorly suited to controlled analysis.

These challenges motivate the need for a controlled and interpretable validation framework capable of reproducing the main physical mechanisms governing solar observability. In this context, simulation enables repeatable testing under controlled conditions, progressive evaluation under degraded sensing, and systematic comparison between navigation strategies. It is therefore particularly relevant for proof-of-concept development prior to full hardware integration.

This work addresses this need by proposing a *physics-based radiometric simulator* for the validation of solar localization and passive heading correction in off-road navigation. The framework is designed as a deterministic physical modeling chain linking astronomical solar position to image-plane observability and navigation-level correction. It integrates solar ephemerides, irradiance modeling, atmospheric transmittance and visibility degradation, fisheye projection, and an approximate sensor response to generate physically consistent observations.

The proposed simulator enables the analysis of navigation resilience under degraded sensing conditions, including GNSS outages and IMU drift. Solar observations act as a passive absolute reference to periodically constrain heading estimates. Rather than aiming at photorealistic rendering, the framework adopts a parametric formulation that favors interpretability and reproducibility, making it suitable as a proof-of-concept validation tool.

The contributions of this paper are summarized as follows:

- A deterministic physics-based simulation framework for validating solar-aided heading correction in off-road navigation.
- A coupled radiometric and geometric modeling chain linking solar ephemerides, atmospheric transmittance, and fisheye image formation.
- A parametric environmental degradation model for controlled evaluation under reduced visibility and sensing uncertainty.
- A navigation-oriented validation methodology for assessing passive heading correction under simulated GNSS and

IMU degradation.
- A proof-of-concept analysis highlighting both the potential and limitations of simulation-based validation for low-cost celestial navigation.

The remainder of this paper is organized as follows. Section II reviews related work on solar-based localization, vision-based orientation estimation, and physics-based modeling approaches. Section III presents the proposed methodology, including the physics-based radiometric modeling, inverse solar localization, and heading correction formulation. Section IV describes the simulation scenarios, evaluation protocol, and experimental results, with a detailed analysis of temporal and spatial heading errors. Finally, Section V concludes the paper and outlines future research directions.

II. Related Works

Existing approaches to solar-based orientation estimation can be broadly categorized into sensor-based, vision-based, learning-based, and physics-based methods.

Early systems in spacecraft guidance and planetary robotics relied on dedicated sun sensors and star trackers capable of providing high-precision directional measurements under controlled radiometric assumptions [1], [2]. While these systems provide accurate and reliable measurements, they require specialized hardware and are not always suitable for low-cost or embedded terrestrial robotic platforms.

A second class of approaches leverages vision-based sky observation to extract global orientation cues. These include polarization-based sky compasses inspired by biological navigation, ephemeris-constrained visual compass formulations, and heuristic solar detection strategies based on intensity maxima or thresholded bright-region extraction [1]–[3]. Although computationally efficient and easy to implement, these methods rely on simplified photometric assumptions that are often violated in real-world environments.

In practice, the appearance of the sky and the spatial distribution of solar radiance are strongly affected by atmospheric and optical phenomena. Cloud occlusions, aerosol scattering, and variations in atmospheric transmittance can significantly alter radiometric conditions [4]–[6]. In addition, geometric distortions introduced by wide-angle and fisheye lenses further complicate the mapping between the solar direction and its image projection [7]–[10]. As a result, intensity-driven heuristics often exhibit limited robustness and may lead to unstable detections or large localization errors under degraded visibility conditions [2], [11], [12].

To improve robustness, learning-based approaches have been investigated, particularly in the context of sky imaging and solar irradiance forecasting. These methods typically rely on supervised segmentation or classification techniques to identify cloud regions or infer the position of the Sun [13]. While they can achieve strong empirical performance, they require annotated datasets, may suffer from limited generalization across different sensors and atmospheric conditions, and reduce interpretability in safety-critical navigation systems.

In parallel, physics-based modeling has been extensively used in atmospheric imaging and computer vision for radiometric calibration, sky rendering, and solar position estimation [7], [8], [14]. These approaches rely on forward models that describe the formation of sky radiance as a function of solar position, atmospheric properties, and sensor characteristics. However, such models are primarily used for simulation or calibration purposes, and their integration into inverse perception frameworks for real-time solar localization and heading estimation remains limited, particularly in the context of wide-field fisheye imaging.

III. Methodology

A. Problem Formulation

The objective of this work is to estimate and correct the vehicle heading by exploiting the observable solar radiometric signature in wide-field fisheye imagery under degraded sensing conditions. Unlike conventional vision-based localization approaches relying on scene features, the proposed method uses the Sun as an absolute celestial reference for orientation correction. The problem is formulated as an inverse estimation task driven by a physics-based forward image formation model.

1) Forward Model of Solar Observation: Let

$$\mathbf{u} = (u, v) \in \Omega \subset \mathbb{R}^2$$

denote pixel coordinates in the fisheye image plane. The observed irradiance distribution is modeled as

$$I_{\text{obs}}(\mathbf{u}) = \mathcal{F}\left(\mathbf{s}_\odot, R, \xi\right) + \epsilon(\mathbf{u}), \tag{1}$$

where $\mathcal{F}(\cdot)$ denotes the non-linear physics-based image formation model, $\mathbf{s}_\odot$ is the solar direction obtained from astronomical ephemerides, $R \in SO(3)$ represents the vehicle-to-world orientation transformation, ξ denotes the set of environmental and instrumental parameters, and $\epsilon(\mathbf{u})$ accounts for residual unmodeled effects. In the current implementation, roll and pitch angles are assumed to be observable through inertial sensing, while the dominant estimated component of R corresponds to the heading correction about the vertical axis.

The parameter set ξ includes atmospheric transmittance, spectral solar irradiance, camera spectral response, optical attenuation (as illustrated in Fig. 1), and visibility constraints. The spatial distribution of irradiance is centered around the projected solar location $\mathbf{u}_\odot$. The residual term $\epsilon(\mathbf{u})$ accounts for sensor noise, cloud occlusions, atmospheric scattering uncertainties, saturation artifacts, lens flare, and calibration residuals.

The forward model combines astronomical prediction of the solar position, atmospheric attenuation, fisheye projection geometry, spectral integration through the camera response, and spatial diffusion induced by optical blur and sensor response. The spatial irradiance distribution is centered around the projected solar location $\mathbf{u}_\odot$ obtained through the fisheye projection model:

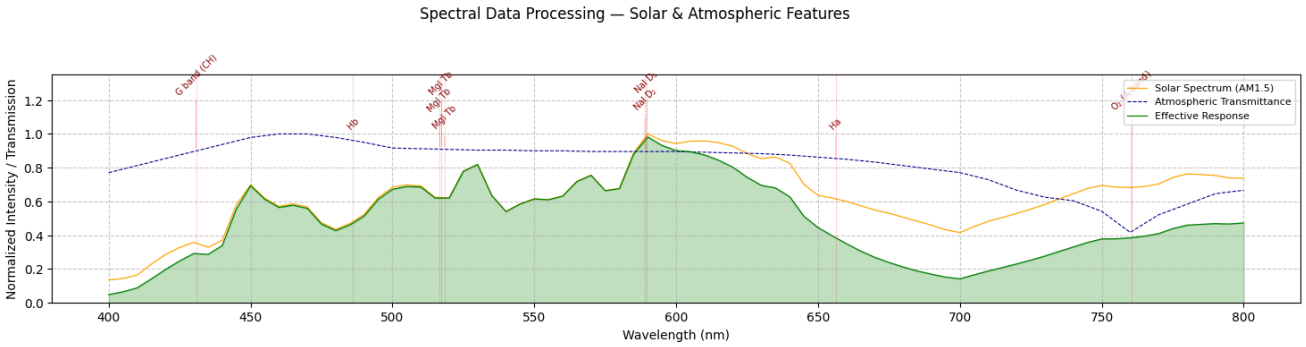


Fig. 1. Spectral weighting of solar irradiance by atmospheric transmittance and imaging sensor response.

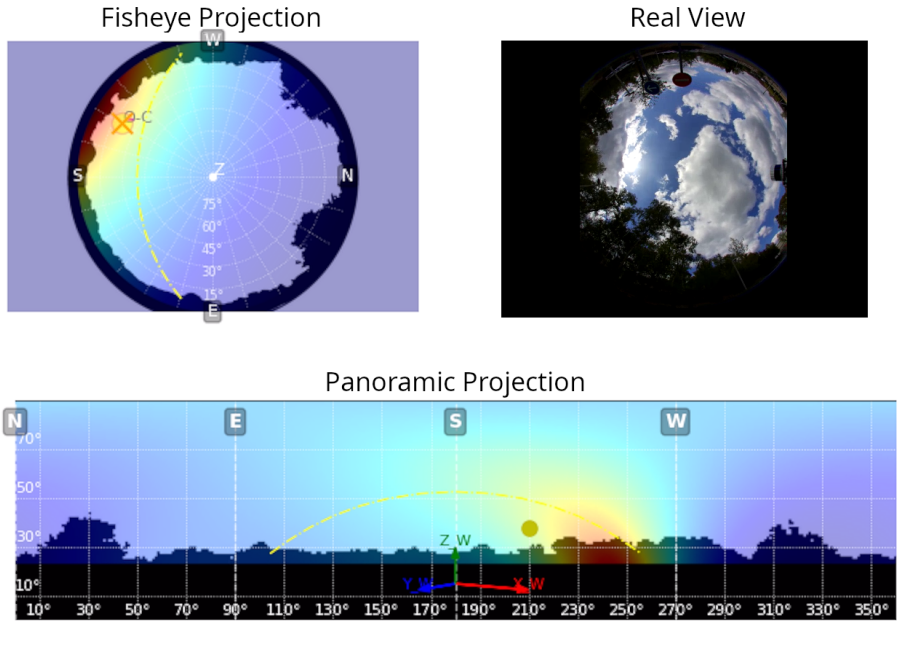


Fig. 2. Illustration of solar direction projection and angular irradiance distribution in the fisheye image plane.

$$\mathbf{u}_{\odot} = \Pi_{\text{fisheye}}\left(R\,\mathbf{s}_{\odot}\right), \tag{2}$$

where $\mathbf{s}_{\odot}$ denotes the unit solar direction vector expressed in the world frame and $\Pi_{\text{fisheye}}(\cdot)$ represents the calibrated fisheye projection operator. The resulting geometric relationship between the solar direction, camera frame, and fisheye image plane is illustrated in Fig. 2. A small drift is visible due to the uncalibrated model under simulation.

2) Inverse Orientation Estimation: Given the observed irradiance distribution I_{obs}, the objective is to estimate the orientation correction maximizing the consistency between the measured fisheye image and the physically predicted solar irradiance distribution. Since the solar direction is known from ephemerides, the inverse problem primarily consists in estimating the orientation transformation that best aligns the predicted and observed solar signatures. The predicted solar irradiance distribution generated by the forward model is then compared to the observed fisheye image in order to estimate the orientation correction minimizing their discrepancy.

The inverse estimation problem is formulated as

$$\hat{R} = \arg\min_{R}\ \mathcal{L}\left(I_{\text{obs}}, \mathcal{F}\left(\mathbf{s}_{\odot}^{\text{pred}}, R, \xi\right)\right), \tag{3}$$

where $\mathbf{s}_{\odot}^{\text{pred}}$ denotes the predicted solar direction obtained from astronomical ephemerides and $\mathcal{L}(\cdot)$ is a discrepancy measure evaluating the consistency between observed and modeled irradiance distributions.

The loss formulation integrates radiometric consistency, geometric coherence, and visibility constraints in order to ensure robust orientation estimation under varying atmospheric and environmental conditions.

In practice, rather than solving this optimization explicitly, the estimation is approximated through a confidence-weighted spatial aggregation in the image plane:

$$\mathbf{u}_{\text{est}} = \frac{\sum_{\mathbf{u}\in\Omega} w(\mathbf{u})\,\mathbf{u}}{\sum_{\mathbf{u}\in\Omega} w(\mathbf{u})}, \tag{4}$$

where the weighting function $w(\mathbf{u})$ encodes the likelihood of each pixel belonging to the solar region. This weight combines radiometric intensity, visibility confidence, and spatial consistency with the predicted solar location.

The estimated pixel location $\mathbf{u}_{\text{est}}$ is then mapped back to a unit direction vector $\hat{\mathbf{s}}_{\odot}$ using the inverse fisheye projection model.

B. Solar-Based Heading Correction

Let $\mathbf{s}_{\odot}^{\text{pred}}$ denote the predicted solar direction derived from ephemerides and the current vehicle state estimate. The discrepancy between predicted and observed solar directions is interpreted as a heading error.

Assuming that roll and pitch are known from inertial sensing, the heading correction $\Delta\psi$ can be approximated from the azimuthal difference:

$$\Delta\psi = \text{wrap}\big(\phi_{\odot}^{\text{est}} - \phi_{\odot}^{\text{pred}}\big), \tag{5}$$

where $\phi_{\odot}^{\text{est}}$ and $\phi_{\odot}^{\text{pred}}$ denote the estimated and predicted solar azimuth angles, respectively, and $\text{wrap}(\cdot)$ ensures angular consistency in $[-\pi, \pi]$.

This correction term is then integrated into the navigation estimator to compensate for heading drift during GNSS outages or inertial degradation.

This formulation establishes a direct link between physical modeling of solar irradiance, image-based observation, and navigation-level correction. By interpreting solar localization as an inverse problem constrained by a physics-based forward model, the proposed approach ensures both interpretability and robustness under degraded visibility conditions.

IV. Simulation Scenarios and Validation Results

A. Simulation Setup

The proposed framework is evaluated within a controlled simulation environment designed to reproduce representative off-road navigation conditions. The simulator generates vehicle trajectories, corresponding ground-truth headings, and associated solar observations under varying environmental configurations.

The simulation integrates deterministic solar positioning based on astronomical ephemerides, fisheye-based observation modeling, and parametric atmospheric degradation, including clear sky and reduced visibility conditions.

To assess navigation robustness, failure scenarios are introduced in the form of abrupt GNSS outages and progressive IMU drift. GNSS outages are simulated by disabling GPS measurements in the navigation pipeline, resulting in inertial-only propagation affected by cumulative drift. These conditions are representative of realistic failure modes in low-cost navigation systems. Figure 3 illustrates a representative snapshot of the simulated navigation scenario. The planned trajectory, ground-truth trajectory, and estimated trajectory are shown together with inertial and GPS measurements. The figure also highlights the simulated solar observation process. The predicted solar direction is projected into the scene, and the corresponding line of sight is used to estimate heading correction. The angular discrepancy between the estimated and expected solar direction is explicitly visualized, along with an associated confidence measure.

This representation provides an intuitive understanding of how solar observations interact with the navigation pipeline. In particular, it shows how solar-based corrections are derived from geometric and radiometric modeling, and how they contribute to reducing heading error in the presence of sensor degradation.

B. Evaluation Protocol

The evaluation focuses on comparing heading estimation performance under two configurations:

- **Baseline navigation:** inertial propagation without solar correction;
- **Solar-aided navigation:** heading estimation corrected using simulated solar observations.

Performance is assessed using the angular error between estimated and ground-truth heading. The following metrics are considered:

- temporal evolution of heading error,
- spatial distribution of error along the trajectory,
- mean and dispersion of angular error.

This protocol enables a direct and controlled comparison of navigation behavior with and without solar-based correction under identical simulated conditions.

C. Temporal Behavior of Heading Error

Fig. 4 shows the temporal evolution of the absolute heading error for both configurations.

Without solar correction, the heading error increases progressively due to inertial drift and exhibits large transient deviations. In contrast, solar-aided correction introduces periodic absolute orientation updates that constrain drift accumulation and maintain a bounded error over time.

Although solar correction is not continuously available due to visibility constraints, it significantly reduces long-term drift by providing intermittent absolute heading updates. These results confirm the role of solar observations as a passive absolute reference that stabilizes heading estimation in degraded sensing conditions.

D. Spatial Error Distribution and Hotspot Analysis

To complement the temporal analysis, the spatial distribution of heading error is examined along the trajectory using a filtered error representation.

Initial trajectory visualizations show that high-error regions are primarily located at trajectory turning points. This behavior is expected, as heading estimation becomes more uncertain during rapid direction changes due to the need to realign the vehicle orientation.

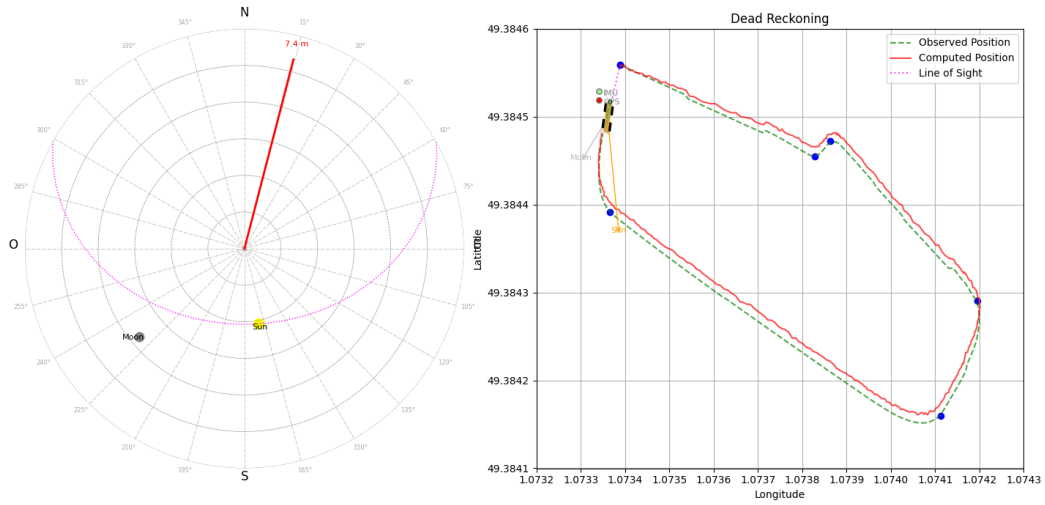


Fig. 3. Overview of the simulated dead-reckoning navigation scenario. The observed trajectory (green dashed) and computed trajectory (red solid) are displayed together with the IMU positions and solar-based orientation information. The polar representation illustrates the estimated solar direction and distance, while the geographic trajectory plot highlights the consistency between observed and estimated vehicle motion within the navigation framework.

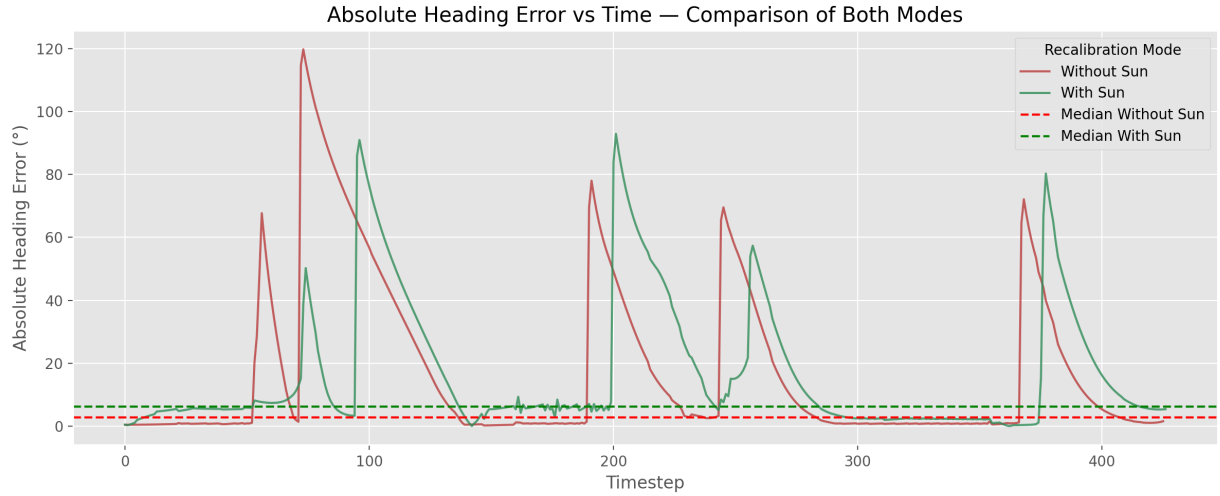


Fig. 4. Temporal evolution of absolute heading error for inertial-only navigation (red) and solar-aided correction (green). Without correction, heading error exhibits significant drift and large deviations. Solar observations provide intermittent absolute orientation updates that reduce error accumulation and improve overall stability.

However, in order to isolate persistent estimation errors, a simple angular filtering strategy is applied. The variation of heading between consecutive trajectory points is computed, and segments exhibiting large angular changes (above a predefined threshold, set to 30° in our experiments) are excluded from the analysis. The remaining samples therefore correspond to regions where the heading error is not dominated by dynamic motion effects, but rather by estimation inaccuracies.

As shown in Fig. 5, spatial analysis highlights that heading errors are not uniformly distributed along the trajectory but are strongly correlated with dynamic maneuvers. In particular, turning regions represent critical conditions where heading estimation is most sensitive to drift.

Without solar correction, large errors appear in these regions and tend to propagate along the trajectory due to accumulated inertial drift, resulting in extended areas of high deviation.

With solar-aided correction, error peaks are still observed during direction changes, reflecting rapid heading variations. However, these peaks remain more localized and are reduced more quickly after the maneuver. This indicates that solar observations provide effective intermittent corrections that limit error propagation.

Quantitatively, solar-aided correction reduces both the magnitude and the spatial extent of persistent high-error regions compared to inertial-only propagation. This demonstrates improved robustness not only in steady-state conditions but also in recovery from dynamic perturbations.

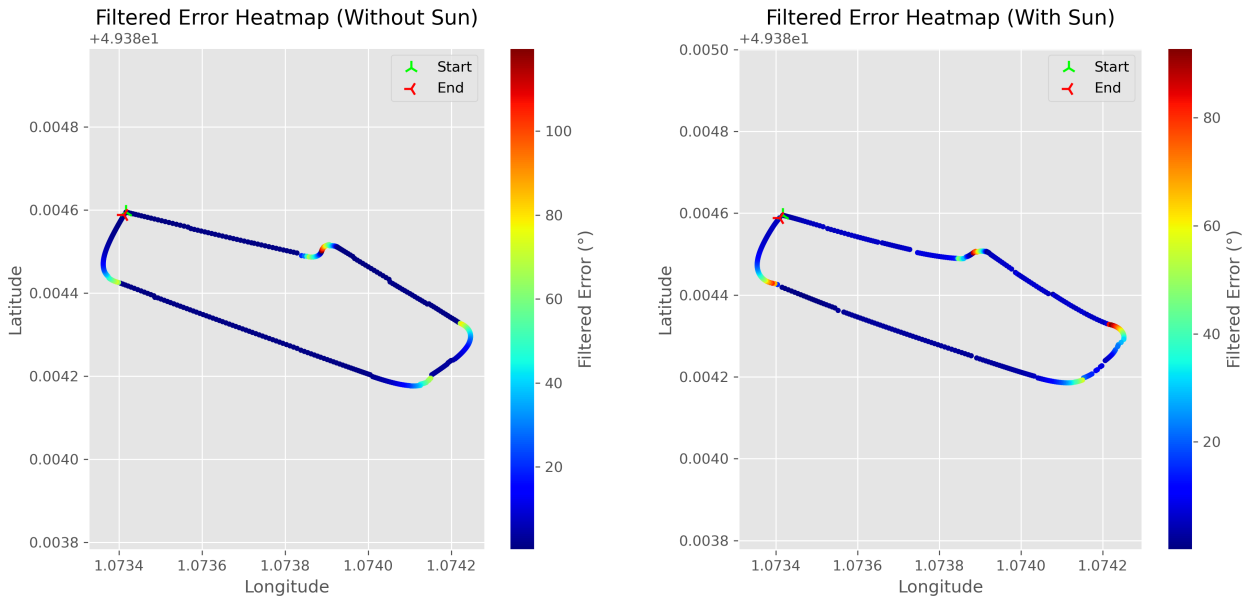


Fig. 5. Spatial distribution of filtered heading error along the trajectory without (left) and with (right) solar-aided correction. High-error regions are primarily concentrated in turning areas. Without correction, errors accumulate and propagate along the trajectory. With solar correction, error peaks remain localized and are reduced more rapidly, highlighting improved recovery after dynamic perturbations.

E. Discussion

The results demonstrate the effectiveness of the proposed simulation framework for evaluating solar-aided navigation under controlled degraded sensing conditions. The deterministic and physics-based formulation enables reproducible analysis of heading behavior in scenarios that are difficult to isolate experimentally.

It is important to note that the simulator relies on parametric approximations of atmospheric effects and does not aim to reproduce fully photorealistic sky imagery. Consequently, the results should be interpreted as a proof-of-concept validation of the navigation principle rather than an absolute performance benchmark.

Despite this limitation, the framework provides a valuable tool for analyzing the interaction between solar observability and heading correction, and for guiding the design of future real-world systems.

V. Conclusion

This paper introduced a physics-based radiometric simulator designed to validate solar-aided heading correction in off-road navigation scenarios. The proposed framework models the complete observation chain, from astronomical solar positioning to image-plane observability, including irradiance, atmospheric transmittance, fisheye projection, and sensor response.

Rather than targeting photorealistic rendering, the simulator adopts a deterministic and parametric formulation that enables controlled, interpretable, and reproducible evaluation of solar observability under varying environmental conditions. This approach allows systematic analysis of navigation behavior in scenarios that are difficult to isolate experimentally, particularly in the presence of GNSS outages and inertial drift.

Simulation results demonstrate that solar observations provide effective intermittent absolute orientation updates, significantly reducing heading error accumulation and improving trajectory consistency. In particular, the analysis of filtered spatial error highlights the ability of solar-based correction to limit error propagation and enhance recovery after dynamic perturbations such as direction changes.

The proposed framework is intended as a proof-of-concept validation tool bridging theoretical solar positioning and navigation-level performance. While the current simulator relies on parametric approximations of atmospheric effects and does not aim at full radiometric accuracy, it provides a coherent and physically grounded basis for evaluating solar-aided navigation strategies.

Future work will focus on improving radiometric fidelity, integrating more realistic atmospheric modeling, and validating the approach with real-world experiments and hardware implementations.

Acknowledgment

The authors gratefully acknowledge the support and technical contributions of the engineers and technicians involved in the MOBILEX Challenge (call proposal by ANR - *Agence Nationale de la Recherche* and AID - *Agence Innovation Defense*, in partnership of CNES - *Centre National d'Etudes Spatiales* and AIT - *Agence Innovation pour les Transports*), in particular Nassim Fouadh, Marc Dehais, Anthony Deshais and Edgard Petit from the Autonomous Navigation Laboratory (ANL), IRSEEM. The authors also gratefully acknowledge Segula Technologies for their support and contribution to

the development of this work. This work was performed, in part, on computing resources provided by CRIANN (*Centre Regional Informatique et d'Applications Numeriques de Normandie*, Normandy, France).

REFERENCES

[1] S. Boucher and C. Macnab, "A review of sun and star tracking systems," *IEEE Access*, vol. 8, pp. 152 594–152 610, 2020.

[2] L. Antonelli *et al.*, "Sun sensor-based heading estimation under cloudy conditions," *IEEE Robotics and Automation Letters*, vol. 6, no. 3, pp. 5191–5198, 2021.

[3] B. Rhodes, "Skyfield: High precision research-grade positions for planets and earth satellites generator," Astrophysics Source Code Library, ascl:19, 2019.

[4] A. Bucholtz, "Rayleigh-scattering calculations for the terrestrial atmosphere," *Applied optics*, vol. 34, no. 15, pp. 2765–2773, 1995.

[5] R. Bird and C. Riordan, "Simple solar spectral model for direct and diffuse irradiance on horizontal and tilted planes at the earth's surface for cloudless atmospheres," *Solar energy*, vol. 36, no. 3, pp. 303–314, 1986.

[6] C. A. Gueymard, "Parameterized transmittance model for direct beam and circumsolar spectral irradiance," *Solar Energy*, vol. 71, no. 5, pp. 325–346, 2001.

[7] S. Dev, F. Savoy, and Y. H. Lee, "Estimating solar irradiance using sky imagers," *Atmospheric Measurement Techniques*, vol. 12, pp. 5417–5429, 10 2019.

[8] A. Hollstein and M. Mauder, "Sun position estimation from all-sky images using physical radiance models," *Atmosphere*, vol. 13, no. 2, p. 318, 2022.

[9] J. Kannala and S. Brandt, "A generic camera model and calibration method for conventional, wide-angle, and fish-eye lenses," *IEEE transactions on pattern analysis and machine intelligence*, vol. 28, pp. 1335–40, 09 2006.

[10] D. Scaramuzza, A. Martinelli, and R. Siegwart, "A toolbox for easily calibrating omnidirectional cameras," *Proceedings of the IEEE/RSJ International Conference on Intelligent Robots and Systems (IROS)*, pp. 5695–5701, 2006.

[11] J. e. a. Redweik, "Sun detection in fisheye images under cloudy conditions using radiometric filtering," *Solar Energy*, vol. 256, pp. 13–25, 2023.

[12] J. Alonso, F. Batlles, C. Villarroel, R. Ayala, and J. Burgaleta, "Determination of the sun area in sky camera images using radiometric data," *Energy Conversion and Management*, vol. 78, pp. 24–31, 2014. [Online]. Available: https://www.sciencedirect.com/science/article/pii/S0196890413006857

[13] Y. Chu, H. T. C. Pedro, L. Nonnenmacher, R. H. Inman, Z. Liao, and C. F. M. Coimbra, "A smart image-based cloud detection system for intrahour solar irradiance forecasts," *Journal of Atmospheric and Oceanic Technology*, vol. 31, no. 9, pp. 1995 – 2007, 2014.

[14] B. Urquhart, B. Kurtz, and J. Kleissl, "Sky camera geometric calibration using solar observations," *Atmospheric Measurement Techniques*, vol. 9, no. 9, pp. 4279–4294, 2016.